A comparative study of reconstruction algorithms for robotic CBCT with various scan trajectories

Seongbon Park ^a, Seungjun Yoo ^a, Junho Lee ^a, Seokwon Oh ^a, and Ho Kyung Kim ^{a,*}
^a Computational X-ray Imaging Laboratory, School of Mechanical Engineering, Pusan Nat'l Univ., Busandaehakro
63beon-gil, Busan 46241

*Corresponding author: hokyung@pusan.ac.kr

*Keywords: Robotic CT system, Metal artifact, Free-form scan trajectory, Reconstruction algorithm

1. Introduction

In modern industrial practice, nondestructive testing (NDT) has become increasingly important for inspecting various components and integrated systems. Among NDT techniques, X-ray inspection is widely used due to its strong penetration power and high spatial resolution. In particular, computed tomography (CT) provides three-dimensional volumetric images with superior spatial and density resolution, making it valuable not only for defect inspection but also for applications across the entire product lifecycle, including design, manufacturing, and maintenance.

However, CT does not always yield satisfactory results. When highly attenuating metallic objects obscure the region of interest, conventional circular or helical CT scan trajectories often generate severe metal artifacts that hinder accurate analysis. To overcome this limitation, robotic CT systems have been developed, where an X-ray source and detector are mounted on a robotic arm with six degrees of freedom, enabling image acquisition along free-form trajectories in 3D space [1]. Such flexibility helps avoid artifact-inducing configurations but inevitably leads to projection inconsistencies.

The Feldkamp–Davis–Kress (FDK) algorithm, the most widely used reconstruction method, assumes data consistency, raising concerns about its effectiveness for non-standard trajectories [2]. In contrast, iterative reconstruction algorithms are known to be more robust against limited data, artifacts, and inconsistencies [3]. This study investigates the performance of different reconstruction algorithms for robotic CT using various scan trajectories to identify the most suitable method for artifact-prone scenarios.

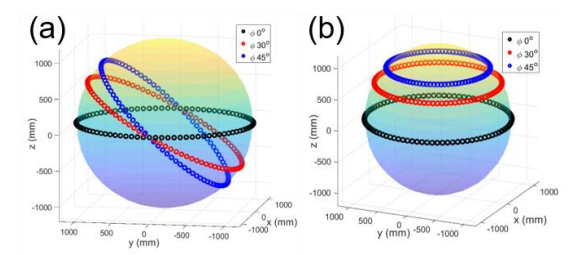


Fig. 1 X-ray source positions depending on the trajectories (a) tilted circular trajectory, (b) offset circular trajectory

2. Methods and Materials

2.1 Experiment

Experiments were performed using a single-arm robotic CT system in which the X-ray source and detector were fixed while the specimen was mounted on the robot arm and rotated [4]. A plastic cylinder containing a postmortem mouse was used as the phantom. To induce metal artifacts, five metallic beads (diameter: 5 mm) were randomly attached to the outer surface of the cylinder. Two scan trajectories were considered: (1) a tilted circular orbit and (2) a circular orbit with different elevations on a spherical surface. The trajectories are illustrated in Fig. 1.

2.2 Image reconstruction

Three trajectories were evaluated: the two circular trajectories shown in Fig. 1 (a) and (b), and a reinforcement learning (RL)-optimized trajectory designed to improve reconstruction quality within the region of interest. For image reconstruction, the analytical FDK algorithm was compared with iterative methods, including SART (simultaneous algebraic reconstruction technique), MLEM (maximum likelihood expectation maximization), and ASD-POCS (adaptive steepest descent projection onto convex sets).

2.3 Evaluation

For performance evaluation, a mouse phantom without

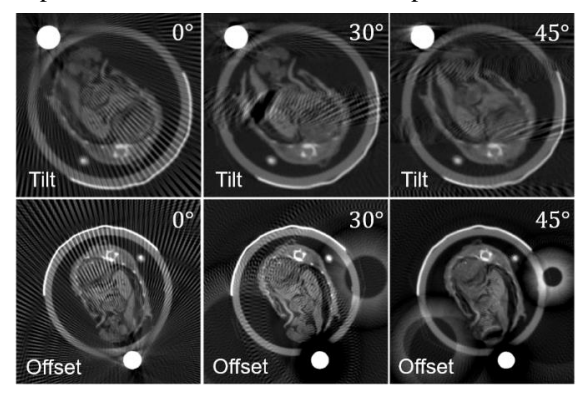


Fig. 2 Reconstructed slice images from CT scans performed with tilted and offset circular trajectories

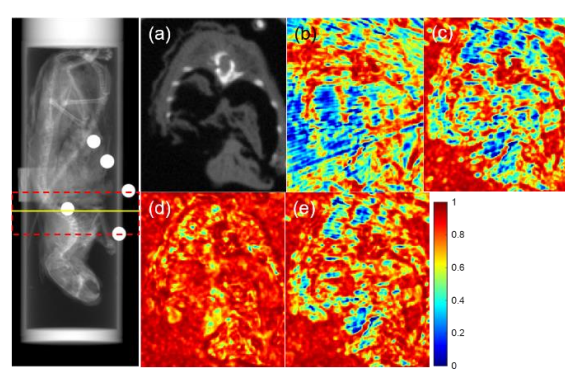


Fig. 3 Projection data and the slice selected for analysis and, (a) reference slice, slice image reconstructed using (b) FDK, (c) SART, (d) MLEM, (e) ASD-POCS

Table. 1 PSNR and SSIM values of reconstructed images for each algorithm

	FDK	SART	MLEM	ASD-POCS
PSNR	36.0721	47.1521	50.0945	48.4370
SSIM	0.5513	0.6609	0.8549	0.7600

metallic beads was scanned from 0° to 359° at 1° intervals, yielding 360 projections. The dataset was reconstructed with FDK to serve as the reference image. Peak signal-to-noise ratio (PSNR) and structural similarity index measure (SSIM) were then calculated for specific slices reconstructed from non-standard trajectories, with higher values indicating better reconstruction quality.

3. Preliminary Results

Fig. 2 shows reconstructed slices using FDK for the trajectories illustrated in Fig. 1. In conventional circular scans, streak artifacts caused by metallic beads severely degraded image quality across the entire slice. In contrast, tilted and offset circular trajectories showed variations in artifact pattern and location depending on trajectory and angle, but demonstrated a significant reduction of global artifacts, particularly in localized regions.

To further compare reconstruction performance against projection inconsistencies and metal-induced artifacts, the RL-optimized trajectory was analyzed using slices heavily affected by artifacts. Fig. 3 presents SSIM maps of reconstructions obtained with FDK, SART, MLEM, and ASD-POCS, along with the reference image. Iterative algorithms exhibited higher PSNR and SSIM values than FDK, with MLEM achieving the highest values among them.

4. Conclusion

This study demonstrated that robotic CT systems with non-standard trajectories can mitigate artifact-inducing factors and improve image quality in regions of interest. While FDK reconstruction suffers from inconsistent data and metal-induced artifacts, iterative algorithms achieved superior results, with MLEM demonstrating the best overall performance. Future work will further

analyze the robustness of MLEM and explore whether FDK can be applied to artifact-free localized regions to balance image quality and computational efficiency.

ACKNOWLEDGEMENTS

This work was supported by the National Research Foundation of Korea (NRF) grant funded by the Korea government (MSIT). (No. RS-2024-00340520).

REFERENCES

- [1] F. Bauer, D. Forndran, T. Schromm and C. U. Grosse, "Practical part-specific trajectory optimization for robot-guided inspection via computed tomography," Journal of Nondestructive Evaluation, Vol. 41, No. 3, pp. 55 (2022)
- [2] L. A. Feldkamp, L. C. Davis and J. W. Kress, "Practical cone-beam algorithm," Journal of the Optical Society of America A, Vol. 1, No. 6 pp. 612-619 (1984)
- [3] M. Beister, D. Kolditz, W. A. Kalender, "Iterative reconstruction methods in X-ray CT," Physica medica, Vol. 28, No. 2, pp. 94-108 (2012)
- [4] S. Park, S. Yoo, J. Lee, S. Oh, H. Kim, and H. K. Kim, "Development of a single-arm robotic computed tomography system," Journal of the Korean Society for Nondestructive Testing, Vol. 45, No. 2, pp. 136–144 (2025)